The Influence of Powder Porosity on the Bonding Mechanism at the Impact of Thermally Sprayed Solid Particles

Article *in* Metallurgical and Materials Transactions A · December 2010
DOI: 10.1007/s11661-010-0488-8

CITATIONS
4

READS
51

3 authors:

Spyros Kamnis
Castolin Eutectic-Monitor Coatings Ltd, UK
35 PUBLICATIONS **424** CITATIONS
SEE PROFILE

Sai gu
Cranfield University
137 PUBLICATIONS **3,643** CITATIONS
SEE PROFILE

Michail Vardavoulias
PyroGenesis SA
100 PUBLICATIONS **763** CITATIONS
SEE PROFILE

The Influence of Powder Porosity on the Bonding Mechanism at the Impact of Thermally Sprayed Solid Particles

SPYROS KAMNIS, SAI GU, and MICHALIS VARDAVOULIAS

High-velocity oxy-fuel (HVOF) thermal spraying can generate dense depositions without melting the powders during spraying. Our previous study showed that most HVOF-sprayed particles are in solid state prior to impact on the substrate. The deposition of solid particles requires sufficient deformation of the particles as a result of a high impact. This report is a continuation of our previous work to study the bonding mechanism for thermally sprayed solid particles. The same hard material, WC-Co powder, is studied by considering the porosity inside the particles. The detailed deposition mechanism is examined by dynamically tracking the particle impingement using finite element analysis (FEA) models. The results confirm that the deposition of high-speed solid particles is caused mainly by the particle deformation and further implies that deformation is enhanced with increase in porosity alone. Therefore, a possible way to increase the deposition efficiency of hard cermet coating could be to use a properly designed porous powder.

DOI: 10.1007/s11661-010-0488-8

I. INTRODUCTION

HIGH-VELOCITY oxy-fuel (HVOF) thermal spraying produces coatings with higher density, superior bond strengths, and less decarburization or oxidation than other high-temperature thermal spray processes, because of its unique advantage of high velocity and low temperature output for sprayed particles. A computational investigation of HVOF sprayed WC-Co particles shows that most particles are in solid state prior to impact.[1,2] The impingement of liquid droplets including spreading, breakup, air entrapment, and solidification has been studied and reported in References 3 and 4, whereas the solid particle impact and its subsequent bonding mechanism are less well understood. Recently, the authors have developed a finite element model to examine the dynamic process of solid particle impingement. A parametric study has been performed to clarify the influence of impact velocity, temperature, particle size, and more importantly, the shape of the particles.[5] Such numerical models provide insights of the high-speed physical process inaccessible by conventional experimental techniques. Experimental results[6] revealed that powder structure, particularly porosity, influences its deformability and, consequently, the deposition behavior of cermet powder such as WC-Co. However, the detailed behavior, including densification and deformation, is not understood clearly for HVOF-sprayed porous powders, because adequate knowledge is lacking about the transition of particles from porous structure to dense deposition layer during impingement. In this article, the previous particle impact model[7] is developed more broadly to investigate the influence of particle porosity in deposition efficiency. The WC-Co powder is used for consistency with the previous study, whereas the particle parameters prior to impact are taken from the computational fluid dynamics (CFD) in-flight particle models reported in Reference 2. The description of the CFD model is not repeated here because it is out of the scope of the current study. An extensive discussion examines the combined effects of strain hardening and thermal softening for different temperatures and velocities. The temperature-dependent critical velocity for successful bonding is derived to take into account particle porosity.

SPYROS KAMNIS, Researcher, and MICHALIS VARDAVOULIAS, Managing Director, are with PyroGenesis S.A., Technological Park of Lavrio, 19500 Lavrio, Greece. Contact e-mail: kamnis@cfd.gr SAI GU, Senior Lecturer, is with the School of Engineering Science, University of Southampton, Highfield, Southampton SO17 1BJ, United Kingdom. Contact e-mail: s.gu@soton.ac.uk

Manuscript submitted April 21, 2010.
Article published online September 30, 2010

II. MODEL DEVELOPMENT

The solid impact dynamics are analyzed by using the finite element commercial solver ABAQUS/Explicit (Dassault Systemes, Suresnes, France). The model accounts for strain hardening, thermal softening, and heating resulting from frictional and plastic dissipation. Because of the small particle size and time scales (nanoseconds) related to HVOF particle impact process, heat transfer from particle to substrate and vice versa can be neglected effectively so heating can be assumed adiabatic.[8,9] The validity of this adiabatic assumption can be assessed by the dimensionless parameter $\frac{x^2}{D\times t}$, where x is a characteristic system dimension, D is thermal diffusivity, and t is the process time. It can be considered as adiabatic heating when $\frac{x^2}{D\times t} \geq 1$. Given $x = 10^{-5}$ m, $D = 10^{-6}$ m^2/s, and $t = 10$ ns, $\frac{x^2}{D\times t}$ is above unity in a typical case of this simulation.

The preceding discussion is based on the solution of the diffusive heat equation. At a small scale, heat conduction is expected to be dominated by a wave propagation mechanism rather than by diffusion. This implies that with the small particle size, the heat propagation would approach the speed of plastic waves and be limited by the speed of sound in the particle. In other words, heat conduction could be even slower than the prediction from the diffusive heat equation for the high-speed impact of small particles. A good description of the preceding argument can be found in References 10–12. The material properties are summarized in Table I.

The cermet microstructure is heterogeneous, especially if the powder is spray dried and sintered. A simplified approach with the "average" properties of the carbide and the cobalt materials are used in the current model for WC-Co powder. Subsequent work will be followed to improve the model with realistic heterogeneous mixtures. The elastic response of the material follows a linear elasticity model, which is adequate for most impact cases. The plastic response of WC-Co is assumed to comply with the widely used Johnson-Cook plasticity model[13] as follows:

Table I. Material Data for WC-Co[17]

Density (kg/m^3)	14,000
Solidus temperature (K (°C))	1580 (1307)
Liquidus temperature (K (°C))	1640 (1367)
Specific heat (J/kg K)	295
Latent heat (J/kg)	420,000
Young's modulus (GPa)	500
Poison's ratio	0.27
Shear strength (MPa)	95

$$\tau = \left(\mathrm{A} + \mathrm{B}\bar{\gamma}_p^n\right) \times \left(1 + \mathrm{C}\ln\frac{\dot{\gamma}}{\dot{\gamma}_0}\right) \times \left[1 - \left(\frac{T - T_0}{T_m - T_0}\right)^m\right] \quad [1]$$

$$T = T_0 + \frac{\beta}{\rho c_p}\int \tau d\bar{\gamma}_p \quad [2]$$

where τ is the flow stress, $\bar{\gamma}_p$ is the average plastic shear strain, $\dot{\gamma}_0$ is the reference shear strain rate, $\dot{\gamma}$ is the imposed shear strain rate, T is the temperature resulting from plastic dissipation, T_0 is the impact temperature, T_m is the melting temperature, β is the work to heat conversion factor (based on the empirical assumption that 90 pct of the kinetic energy is dissipated to heat allowing for heat conduction within the particle), c_p is the heat capacity, ρ is the density, and A, B, C, m, and n are material-dependent constants, such as static shear strength, strain-hardening modulus, strain rate sensitive coefficient, thermal-softening exponent, and strain-hardening exponent, respectively.

The impact process is modeled in a three-dimensional (3-D) domain shown in Figure 1. The substrate dimension is given to be three times larger than the particle diameter to avoid possible effects on the

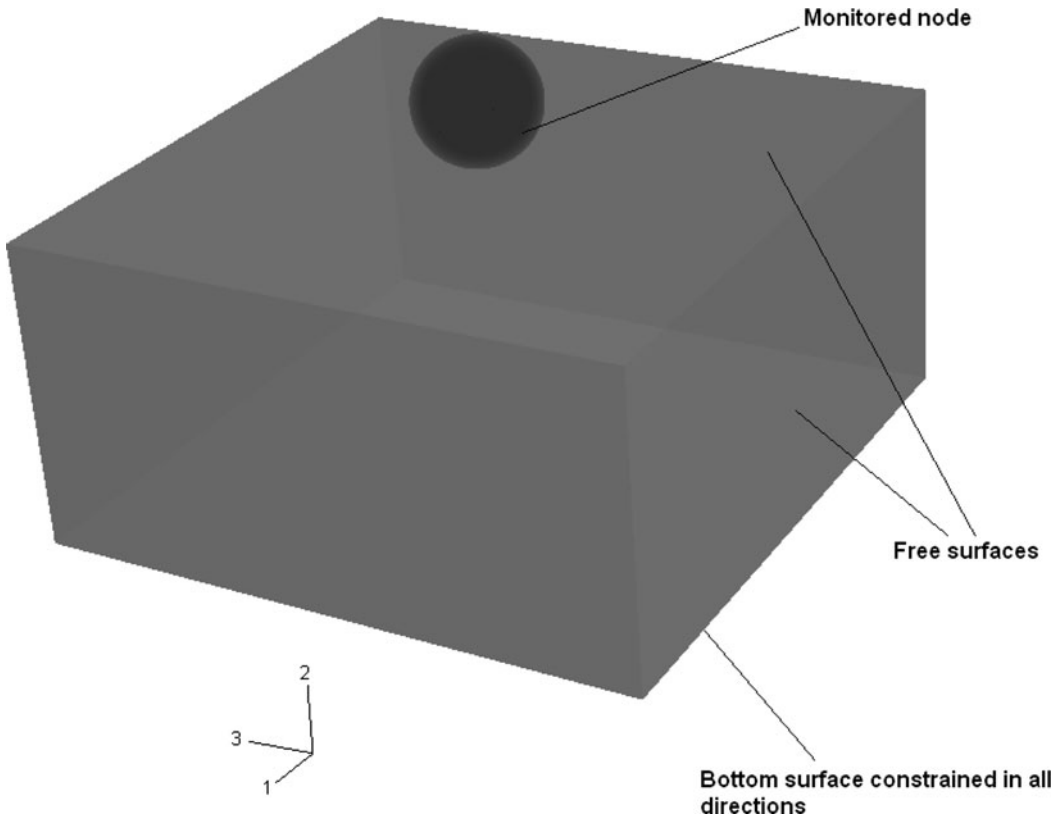

Fig. 1—Computational domain for 3-D finite element model.

particle-substrate deforming zones from the boundary nodes. The substrate bottom face is constrained in all directions, while the other faces are assumed free. Grid sensitivity analyses have shown that the mesh size plays a dominant role on the material heating and consequently to shear flow localization. Further details for grid dependence study including mesh size can be found in Reference 9. The velocity and temperature of spray particles prior to impact are taken from Reference 2 for the chosen diameters. The temperature gradient along the particle radius is neglected, and the whole particle is assumed to be at the same surface temperature without gradient along the particle radius. The current work examines only the influence of porosity on the impact dynamics. The influence of porosity on particle heating will be examined in a future study. When microporosity is present in agglomerated nanostructured powder, the effective thermal conductivity changes with the extent of porosity. As a result, the temperature gradient becomes noticeable and is expected to enhance the deformability of porous particles. The monitor node is selected randomly on the surface of the impacting particle at a location in which intensive plastic deformation is expected and temperature evolution is more pronounced. The monitored node as shown in Figure 1 is used for the output of results concerning temporal evolution of temperature and stress. The selected monitoring node is located on particle's bottom surface where mechanical interlocking with the substrate is taking place. Figure 2 shows the simulated porous structure within the particle, together with a scanning electron microscopy (SEM) image from PyroGenesis S.A metallographic laboratory of the agglomerated nanostructured WC-Co powder. The powder granules are spherical, which ensures good flowability. These powder agglomerates are porous with dispersion of fine carbide particles in the Co matrix. The powder is fabricated by using a proprietary process, in which individual nanoparticles are reconstituted into the spherical micron-size granules for thermal spray. Non-agglomerated nanoparticles cannot be thermal sprayed successfully because of their low mass and difficulty in entraining them into the moving gas stream and depositing onto a substrate.

The model is applicable to heterogeneous materials consisting of randomly oriented and distributed spherical inclusions (or pores) in an elastic-plastic matrix, which in general case, can change their size, shape, and orientation, because of the applied deformation. The plasticity model accounts for uniaxial tension, simple shear, plastic flow localization, and necking in plane strain tension during microstructure evolution. A study of sintered iron powder[14] shows that powder with 3 pct porosity has fully isolated spherical or elliptical pores, and powder with 20 pct porosity has interconnected pores of complex shape. It is difficult to have a good representation of the complex pore structure at high porosity level. This study chooses two porosity levels,

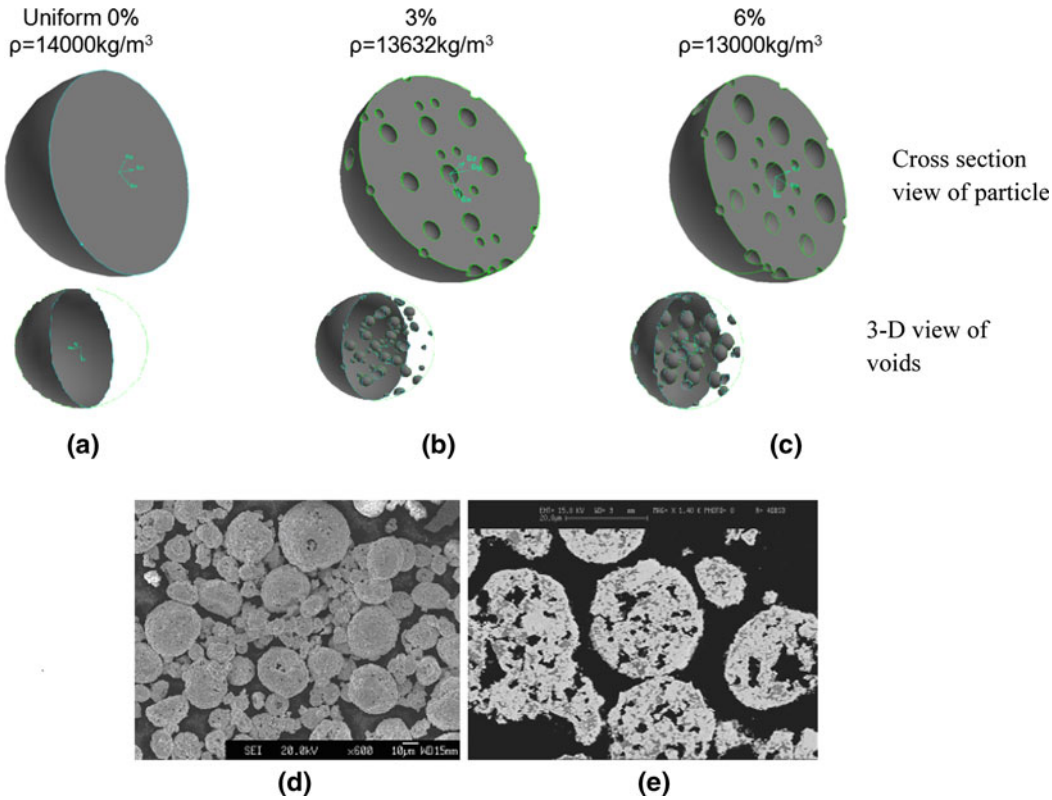

Fig. 2—Microstructure within the particle for (*a*) fully dense, (*b*) 3 pct porosity and (*c*) 6 pct porosity, (*d*) SEM images of the nanostructured WC-Co powder. (*e*) SEM backscattered electron image of cross-sectional view of the powder.

3 pct and 6 pct, which correspond to the reduction of powder volume as a result of the hollow, isolated air voids created within the particle.

III. RESULTS AND DISCUSSION

It is known that, prior to thermal spraying, substrate surfaces are prepared by blasting to enhance bonding. An accurate representation of the real application should have the detailed surface profiles of the substrate, which will require extensive computation with sophisticated geometry and grid. In this work, the substrate is defined as a flat surface with the same property as the WC-Co powder, which can be regarded as the previously formed base coat. The substrate has a uniform temperature of 300 K (27 °C). The particle parameters are varied in terms of particle porosity, impact velocity, and temperature. The 20-μm spherical particles are selected as the baseline particles in this study. The use of WC-Co materials is based on the following assumption.

(1) The particle is assumed to melt when the Co element reaches the liquidus temperature of 1640 K (1367 °C).
(2) Melting is assumed to take place in a thin interfacial region between the particle and substrate. The remained solid particle will deform according to Eqs. [1] and [2]. It is believed that the viscous-type deformation is limited only to the thin region in which mechanical interlocking takes place to enable bonding. The assumption of WC-Co in one state within this thin layer should not make a substantial difference to the overall impact dynamics as verified in Reference 5.

A. *Influence of Particle Porosity on Strain*

The impingement of 6 pct porous particle with a velocity of 500 m/s and temperature of 700 K (427 °C) is illustrated in Figure 3. The particle starts to deform immediately after impact, causing a crater on the substrate. In the early stage of impingement (30 ns), the contact surface deforms and the crater size increases in width and depth to accommodate the deformed particle. At 100 ns, when the particle kinetic energy has decreased to zero, the particle flattens to a lens-like shape. Figure 4 shows the nominal stress–strain curves for particles with different porosity (0 pct, 3 pct, and 6 pct, respectively). Strain hardening is reduced according to porosity, with highest porosity of 6 pct showing lower rate of stress–strain increase, which is an indication toward saturation stress at high porosity levels. In all cases, the compressive response follows the pattern of a power law. The nominal stress–strain curves demonstrate clearly the behavior change from solid to porous materials. The influence of porosity on material strength is represented more accurately using the flow stresses at different strains against porosity. Figure 5 shows the approximate linear function between the flow stress and porosity at equivalent strain levels.

B. *Influence of Particle Porosity on Deformation Mechanism*

The impact process can be divided into three stages: linear elasticity, plateau, and densification. Deformation starts homogeneously immediately after the impact, and then it is localized at the weakest sections and progresses steadily until densification. Figure 6 shows the microstructure of the WC-Co particle after 100 ns. Compared with the predeformation structure, some spherical pores change into an ellipsoidal shape. The pores are still visible, but many have squashed structures. Figure 4 compares the strain distribution at 100 ns for different

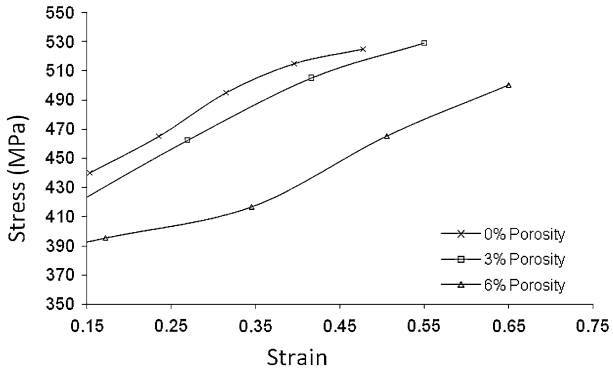

Fig. 4—Stress–strain curves of porous WC-12Co with 0 pct 3 pct, and 6 pct original porosity under dynamic impaction.

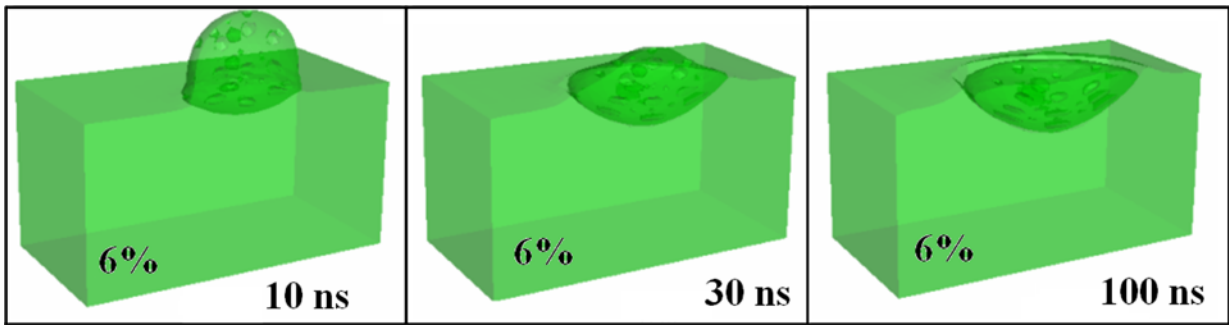

Fig. 3—Time sequence deformation images of a 6 pct porous particle impacting on a substrate with a velocity of 500 m/s and temperature 700 K (427 °C).

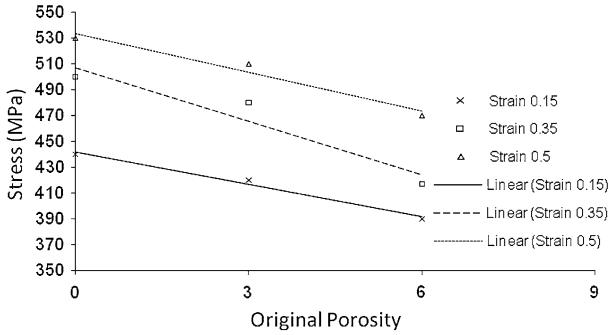

Fig. 5—Equivalent flow stress at different strains against the original porosity of the powder. The stress levels for 0.15, 0.35, and 0.5 strains are taken from Fig. 4.

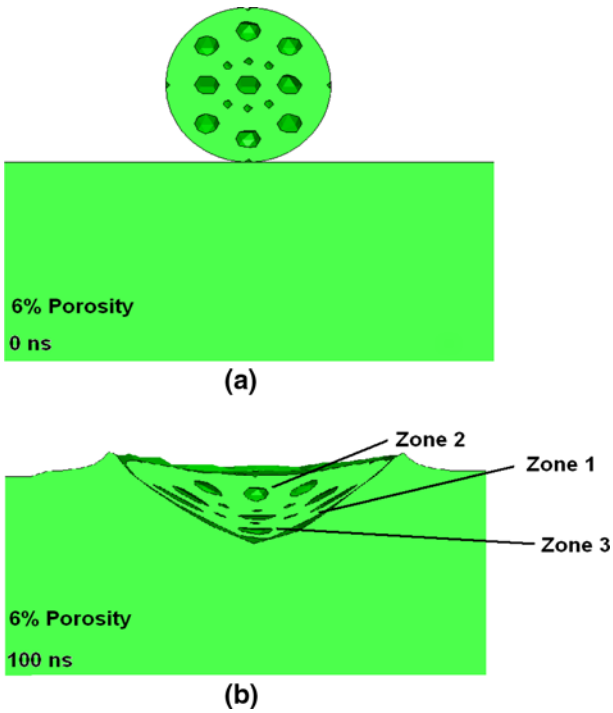

Fig. 6—Porous microstructure deformation images before (top) and after impact (bottom).

porous particles. The maximum strain of the porous particle occurs in zone 1 near the contact surface where the strain decreases toward the particle center, whereas the minimum strain occurs on the top of free surface (zone 2). This is caused by stress and results in volumetric strain in the porous particles, which is different from the deformation of the fully solid particles. Solid particles have a decreased strain in all directions, which reduces the extent of flattening. Particle flattening is greatly dependent on normal stress, which decreases from the contact surface to the center. In the contact regions, compressive stress is higher because of impact velocity; hence, the pore structures around those regions are damaged badly as shown in Figure 6. The particle experiences a compression combined with lateral flow; therefore, pores are deformed initially into a lens-like shape (zone 3) and finally to line-like shape in zone 1 at the end of impaction process. The dynamic contact pressure generated on the impact of the particle is concentrated near the interface between the impacting particle and the underlying substrate. The top region of the particle is less influenced by the impact pressure and tends to retain its original structure. Accordingly, the densification of deposited particles during deposition process is only effective in the region near substrate interface as typically shown in Figure 7, zone 1. With regard to porous material, the compressive deformation still occurs mainly near the contact region but spreading is larger as porosity increases as can be seen in Figure 8. This trend can be attributed to the presence of pores, which results in a lower work hardening effect during deformation than that of fully solid material. Moreover, the substrate deforms less as a result of reduced impact from porous particles. Decreased normal stress from the contact surface to the particle center for porous particles, as a result of compaction of air voids, is also a factor that affects deformation levels in both substrate and particle.

C. *Influence of Porosity on Bonding*

The bonding of particles with substrate is attributed mainly to localized thermal buildup during the impact process. Adiabacity quantified by Fourier number[15] is applicable to all powders in the process of deformation, such as dynamic particle compaction. It has been reported that almost 100 pct of the work done during high strain rate deformation is converted to heat.[16]

The reported study on fully solid particles states that the kinetic energy prior to impact is a key factor for strong adhesion.[7] Solely judged on the value of impact velocity, porous powder should form a better coating from the HVOF process.[5] In fact, the particle microstructure influences the rate of deformation rate during impact. Three temperature contour plots are compared in Figure 9, which gives more quantitative examination of the aforementioned deformation trends and their relation to temperature buildup in the interfacial contact region. The particle size is set to 20 μm with different porosity. The particle is assigned the same impact conditions for velocity and temperature of 400 m/s and 700 K (427 °C), respectively. The results show that within the interfacial contact region, the particles reach a lower temperature as porosity decreases. The resistance to the temperature increase is as discussed in the Section III–B. This is caused by the lower levels of plastic deformation at low porosity.

The required deformation and work conversion to heat, which enables the formation of bonding through mechanical interlocking of the particle substrate, is more pronounced in the presence of pores. In this sense, higher impact velocities or temperatures are required for fully solid spherical particles to achieve melting in the same extent as porous particles. For a more quantitative comparison, a point in the maximum deformation area for each particle is selected as illustrated in the black circles in Figure 9. The surge of temperature during the impingement is plotted at those points. The most

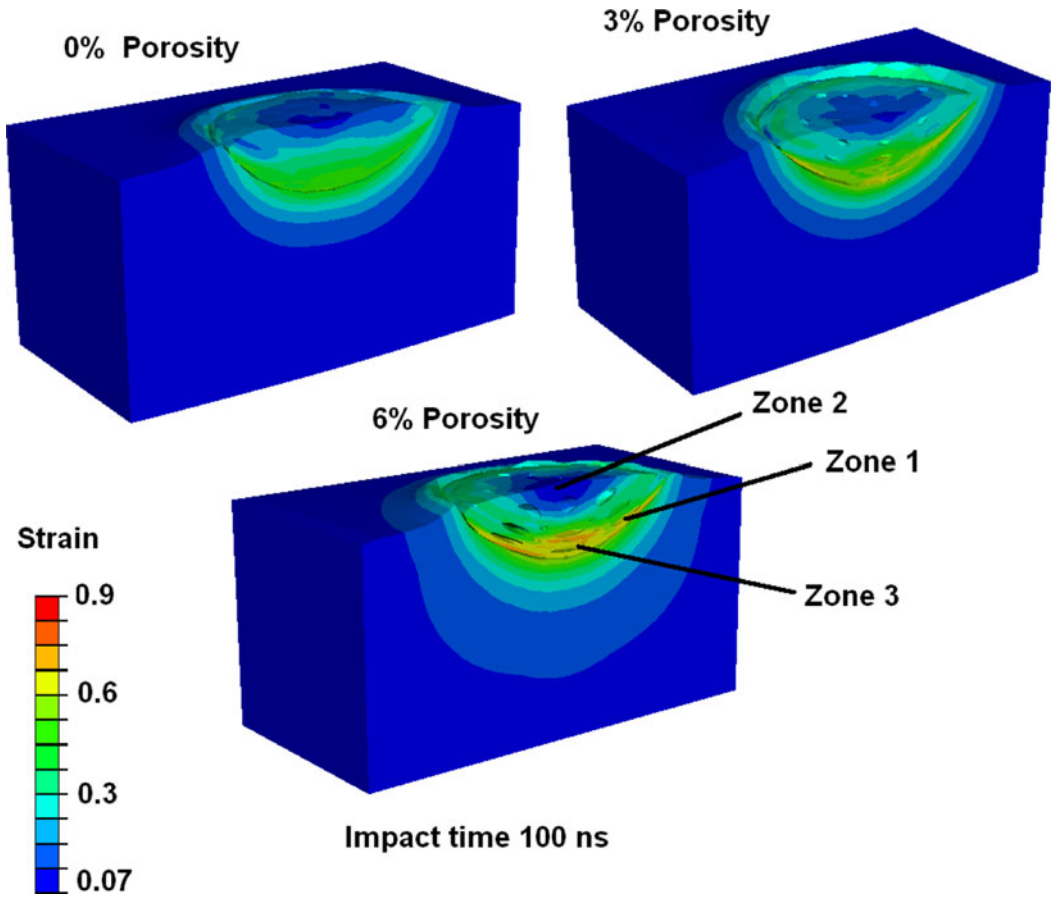

Fig. 7—Contours of strain level at the end of the impaction process for three different porosity levels.

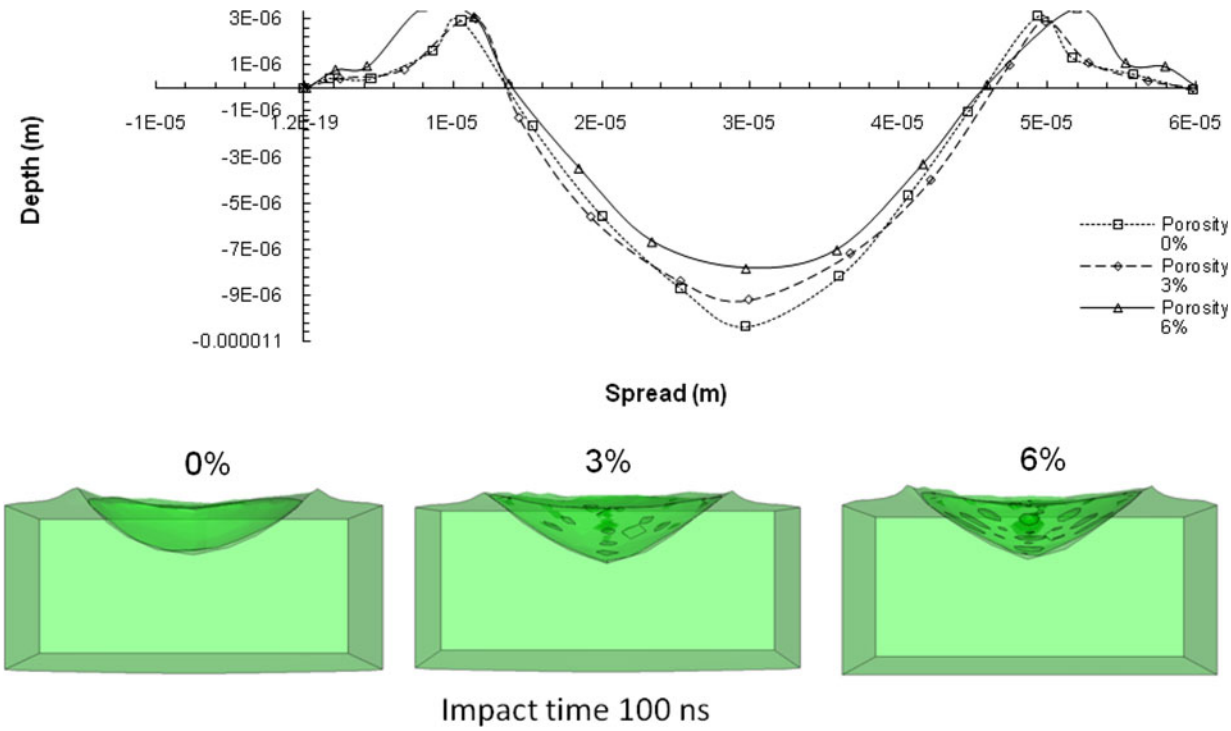

Fig. 8—Particle overall spreading after impact for different porosity levels.

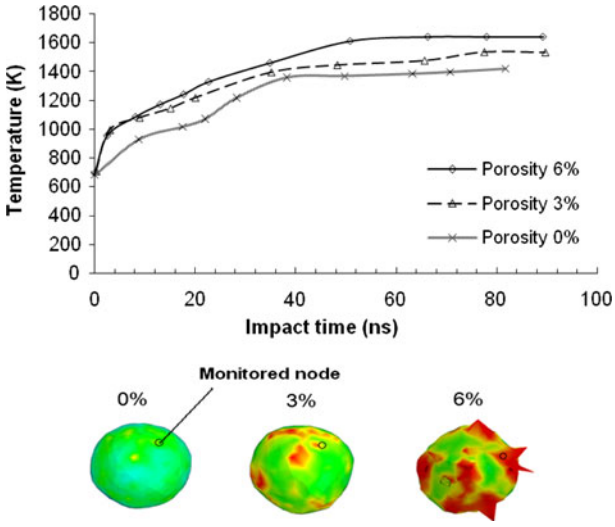

Fig. 9—Surface temperature development during impact.

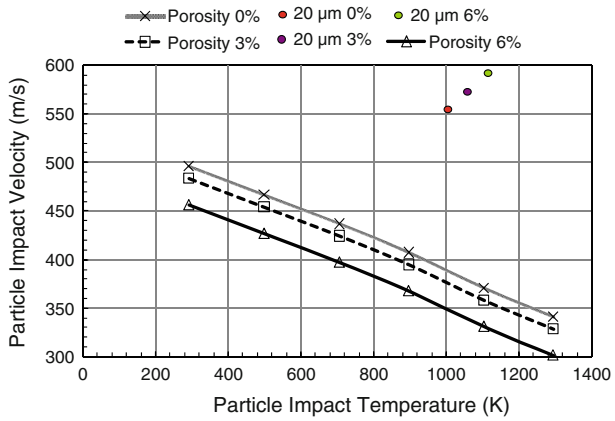

Fig. 10—Critical impact parameters for different porosity 20-μm particles.

substantial increase in temperature occurs at the initial stage of impact, 0–30 ns, where the kinetic energy is at the highest level. The temperature increase stabilizes between 30 ns and 80 ns. From then, a slightly more pronounced temperature rise is visible, particularly for 6 pct porous particle. On impact, the kinetic energy of the powder particles is distributed at a molecular level and is dissipated to heat as the particle deforms. The temperature rises as a result of the work done during plastic energy dissipation, which results in a phase change from solid to liquid. The temperature increase is less noticeable as the particle becomes denser because of the different extent of deformation.

D. *Critical Impact Conditions*

It is necessary from a commercial point of view to know the critical impact velocity and temperature for different particle porosities so that an adequate bonding strength and higher deposition efficiency can be obtained. Figure 10 shows the critical velocity as a function of impact temperature for different particles. The results indicate that a proportional increase of impact velocity is required as the particle becomes denser. The points marked with color cycles represent the particle impact velocity and temperature obtained from CFD models for in-flight particle dynamics from HVOF gun.[2] For the particles located above the lines, the impact temperature and velocity are adequate to ensure bonding on the substrate. In the case of the 20-μm particles, sufficient energy is generated for good bonding. The reduction in density influences the inertia of the particles and, consequently, their acceleration. For this reason, porous particles are expected to attain a higher velocity. This may also contribute to a better coating from porous particles. However, porous particles have more complicated surfaces, different effective thermal conductivity, and reduced density, which might increase the complexity of the in-flight particle dynamics. To improve our understanding of thermally sprayed porous particles, more accurate quantitative analyses are required by using CFD and online diagnostics.

IV. CONCLUSIONS

A finite element analysis model has been developed to study the impingement process of solid particles and the bonding mechanism between the particle and substrate. The results provide insights into the intricate interaction between plastic deformation and bonding formation. A summary of conclusions is as follows:

1. The deformation rate of the particle during impact plays a dominant role in particle stress localization and melting of the interfacial region. Fully dense particles require more kinetic and thermal energy for good adhesion on the substrate.
2. The porosity level of spherical particles affects positively the plastic deformation rate and, consequently, the bond strength that gives less complexity for spraying porous powder. The deformation behavior of porous powder during HVOF spray is characterized by an increase of particle spreading as porosity increases. This trend can be attributed to the decreased normal stress from contact surface to particle center and the smaller work-hardening effect because of the porous microstructure.
3. The pores are squashed, or even disappear, near the particle substrate region because of the high pressure on impact. The pores are deformed into lens-like or line-like shapes in combination with the particle flattening of the particle volume.
4. The results obtained with the model are consistent with the observations in the experimental studies[6] that powder porosity can enhance the deposition efficiency of hard cermet coating.

REFERENCES

1. N. Zeoli, S. Gu, and S. Kamnis: *Int. J. Heat Mass Transfer*, 2008, vols. 15–16, pp. 4121–31.
2. S. Kamnis, S. Gu, T.J. Lu, and C. Chen: *Comput. Mater. Sci.*, 2008, vol. 43, pp. 1172–82.

3. S. Kamnis and S. Gu: *J. Phys. D: Appl. Phys.*, 2005, vol. 38, pp. 3664–73.
4. S. Kamnis, S. Gu, T.J. Lu, and C. Chen: *J. Phys. D: Appl. Phys.*, 2008, vol. 41, pp. 165303–10.
5. S. Gu and S. Kamnis: *Metall. Mater. Trans. A.*, 2009, vol. 40A, pp. 2664–73.
6. P.H. Gao, Y.G. Li, C.J. Li, G.J. Yang, and C.X. Li: *J. Therm. Spray. Technol.*, 2008, vol. 17 (5–6), pp. 742–49.
7. S. Kamnis, S. Gu, T.J. Lu, and C. Chen: *Comput. Mater. Sci.*, 2009, vol. 46, pp. 1038–43.
8. M. Grujicic, J.R. Saylor, D.E. Beasley, W.S. DeRosset, and D. Helfritch: *Appl. Surf. Sci.*, 2003, vol. 219, pp. 211–23.
9. H. Assadi, F. Gartner, T. Stoltenhoff, and H. Kreye: *Acta Mater.*, 2003, vol. 51, pp. 4379–94.
10. D.Y. Tzou: *J. Heat Transfer*, 1995, vol. 117, pp. 8–16.
11. G.S. Prakash, S.S. Reddy, S.K. Das, T. Sundararajan, and K.N. Seetharamu: *Num. Heat Transfer A*, 2000, vol. 38, pp. 513–32.
12. R. Kapoor and S. Nemat-Nasser: *Mech. Mater.*, 1998, vol. 28, pp. 1–12.
13. G.R. Johnson and W.H. Cook: *Proc. 7th Int. Symp. Ballistics*, The Hague, The Netherlands, 1983, pp. 541–48.
14. H. Danninger, G. Jangg, B. Weiss, and R. Stickler: *Powder Metall. Int.*, 1993, vol. 25, p. 170.
15. O. Roman, A. Mirilenko, and I. Pikus: *Sov. Powder Metall.*, 1990, vol. 28, pp. 840–45.
16. R. Kapoor and S. Nemat-Nasser: *S. Mech. Mater.*, 1998, vol. 27, pp. 1–6.
17. E. Aldie and Johnson, Jr.: *Technical Note 3309*, National Advisory Committee for Aeronautics, Washington, DC, 1954.